

Suppression effect of liquid composition on defiltration of nanofluids in lyophobic environment

A Han and Y Qiao¹

Department of Structural Engineering, University of California at San Diego, La Jolla, CA 92093-0085, USA

E-mail: yqiao@ucsd.edu

Received 13 March 2007, in final form 14 March 2007

Published 18 May 2007

Online at stacks.iop.org/JPhysD/40/3436

Abstract

Understanding nanofluidic behaviours in energetically unfavourable confining environments is essential for the development of high-performance nanoporous energy absorption systems. In the current study, the effect of liquid composition on defiltration in a hydrophobic nanoporous silica gel is investigated experimentally using two types of admixtures: carbamide of a relatively small molecular size and sodium bis(2-ethylhexyl) sulfosuccinate of a relatively large molecular size. By adding carbamide in the liquid phase, while the change in the solid–liquid interfacial tension is secondary, the defiltration volume can be lowered significantly, which can be related to the difficulties in gas phase formation and growth in nanopores. The factor of sodium bis(2-ethylhexyl) sulfosuccinate comes in mostly by affecting the liquid motions in relatively small nanopores.

1. Introduction

For more than a decade, nanofluidic behaviour has been an active research area [1–3], which has provided a scientific basis for the development of micro- and nanofabrication, biomedical, selective absorption and adsorption, intelligent catalysis, and advanced materials processing technologies. Recently, the motions of confined liquids in energetically unfavourable nanoenvironments, e.g. in lyophobic nanoporous materials, have attracted considerable attention [4–8]. For instance, by applying an external pressure, water can be forced into a hydrophobic nanoporous material. Simulation work was reported for carbon nanotubes [9, 10].

In certain types of nanoporous materials, particularly in mesoporous materials of nanopore sizes in the range 2–50 nm, the confined liquid consists of a reversible part and an irreversible part [11]. Upon removal of the external pressure, only the reversible part can defiltrate out of the nanopores, and the irreversible part is ‘locked’ inside; that is, the excess solid–liquid energy cannot be fully released. The reversible part is the liquid confined in the smallest nanopores, and the irreversible part is the liquid confined in the relatively large

nanopores. These materials can be used to develop high-performance nanoporous energy absorption systems (NEASs). Due to the ultrahigh surface area of the nanoporous material, the efficiency of the energy transformation from mechanical pressure to solid–liquid interfacial tension is typically at the level of 10 J g^{-1} , much higher than that of conventional energy absorbing materials such as reinforced polymers and shape memory alloys.

The factors that govern the performance of a NEAS include the infiltration pressure, p_{in} , the infiltration volume, V_{in} , the defiltration pressure, p_{d} , and the defiltration volume, V_{d} , where p_{in} is the pressure at the onset of infiltration when the capillary effect is overcome, V_{in} is the accessible nanopore volume during infiltration, p_{d} is the pressure at which defiltration starts and V_{d} is the amount of the reversible part of confined liquid that can come out of the nanopores as the pressure is lowered. As depicted in figure 1, as a pressure is applied on a system consisting of a nanoporous material immersed in a nonwetting liquid, following the initial linear compression stage (*OA*), as the external pressure, p , reaches p_{in} , the liquid is forced into the nanopores, accompanied by the formation of the infiltration plateau (*AB*) of the width of V_{in} . As the pressure is lowered, due to the difficulties in ‘outflow’, defiltration would not take place until the pressure is reduced to

¹ Author to whom any correspondence should be addressed.

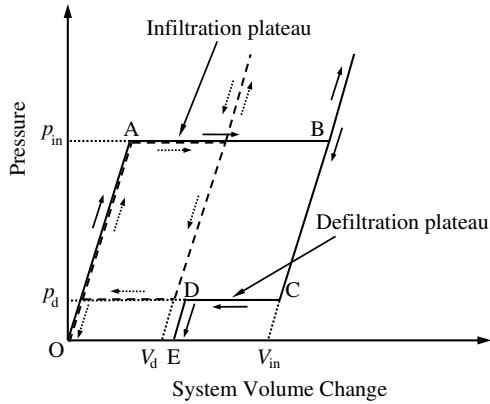


Figure 1. A schematic diagram of the sorption isotherm curves of a NEAS. The solid line indicates the first loading–unloading cycle and the dashed line indicates the second loading–unloading cycle.

p_d , followed by the formation of the defiltration plateau (CD) of the width of V_d . Since, after the first loading–unloading cycle, the irreversible part of confined liquid remains in the nanopores, in the second cycle the width of the infiltration plateau would be decreased to V_d . The energy absorption efficiency of the NEAS can be assessed as $\Delta E = p_{in} \cdot V_{in} - p_d \cdot V_d$.

To avoid harmful ‘blast lung’ problems caused by stress waves under high-strain-rate loadings [12–14], V_d needs to be minimized. In previous studies, it was reported that using admixtures in liquid phases can result in considerable changes in p_{in} [15], p_d [16] and V_{in} [17], while the studies on V_d are scarce. In the current study, we investigate the effects of addition of carbamide and sodium bis(2-ethylhexyl) sulfosuccinate. The experimental data show that both of them can significantly lower V_d , while the mechanisms are different. The former affects V_d by influencing the energy barrier of gas phase nucleation, and the dominant factor of the latter is related to the blocking effect.

2. Experimental

Two types of admixtures were investigated. One was Sigma U5378 carbamide, with the molecular formula of NH_2CONH_2 , the molecular weight of 60.06 and the molecular size of about 0.3 nm, and the other was Sigma D1685 sodium bis(2-ethylhexyl) sulfosuccinate (SBS), with the molecular formula of $\text{C}_{20}\text{H}_{37}\text{NaO}_7\text{S}$, the molecular weight of 444.56 and the molecular size of about 2 nm. Both of them are surfactants that can be dissolved easily in water. As carbamide is added in water, with the two polar amino groups in its molecule, molecular clusters of gas and liquid species can be formed more easily by hydrogen bonds, and therefore the gas solubility increases. SBS is a long chain molecular, with the chain length comparable to the nanopore size. With the two ethyl groups on both sides of the chain, it can block the nanopore.

After adding the admixtures in 7 g of distilled water, the liquid was mixed with 0.5 g of Fluka 100 C_8 reversed phase end-capped silica gel and placed in a steel cylinder. The silica gel was degassed at 150 °C for 12 h in a vacuum oven. The admixture concentration was in the range 2–20 wt%. The average nanopore size of the silica gel was 7.8 nm, with the

Table 1. The data of p_{in} , V_{in} , p_d and V_d .

	p_{in} (MPa)	V_{in} ($\text{cm}^3 \text{g}^{-1}$)	p_d (MPa)	V_d ($\text{cm}^3 \text{g}^{-1}$)
Pure water	16.0	0.45	3.5	0.12
10 wt% carbamide	15.6	0.47	3.2	0.04
20 wt% carbamide	14.0	0.48	1.0	0.02
2 wt% SBS	15.0	0.39	2.2	0.06
20 wt% SBS	11.9	0.38	1.8	0.03

standard deviation of 2.4 nm. The specific surface area was $287 \text{ cm}^2 \text{g}^{-1}$, and the specific pore volume was $0.55 \text{ cm}^3 \text{g}^{-1}$.

The mixture of the silica gel and the liquid phase was sealed and compressed by a steel piston quasi-statically in the displacement-control mode using a type 5569 Instron machine. The speed of the piston was kept at 1 mm min^{-1} . After the pressure reached 50 MPa, much lower than the pressure of 500–700 MPa that can cause nanopore collapse, the piston was moved out of the cylinder at the same speed, and thus the system was unloaded. After the pressure was reduced to zero, the loading–unloading procedure was immediately repeated. Table 1 shows the data of p_{in} , V_{in} and p_d , V_d . The starting points of infiltration and defiltration plateaus are defined as the places where the slopes are equal to one-half of that of the initial linear compression section. Figures 2–5 show the measured sorption isotherm curves of systems containing 10.0 wt% carbamide, 20.0 wt% carbamide, 2.0 wt% SBS and 20.0 wt% SBS, respectively. The dashed lines indicate the behaviours of the NEAS based on pure water.

3. Results and discussion

According to figure 2, it is clear that the addition of 10 wt% of carbamide has little influence on the infiltration pressure, $p_{in} = 15.6 \text{ MPa}$, and the infiltration volume, $V_{in} = 0.47 \text{ cm}^3 \text{g}^{-1}$, compared with the pure water-based system ($p_{in} = 16.0 \text{ MPa}$ and $V_{in} = 0.45 \text{ cm}^3 \text{g}^{-1}$). The sorption isotherm curves of the first loading–unloading cycles of the carbamide modified system and the pure water-based system are almost identical, except that for the carbamide modified system p_{in} is slightly lower by about 0.5%, within the uncertainty range of the pressure measurement machine. The value of V_{in} is $0.47 \text{ cm}^3 \text{g}^{-1}$, slightly smaller than the gas absorption measurement result of the specific nanopore volume. Compared with the ‘ideal’ curve shown in figure 1, the slope of the infiltration plateau of the experimental data is finite, which should be attributed to the nanopore size distribution. Since the capillary effect in larger nanopores is easier to overcome, the infiltration begins in the largest nanopores. As the pressure increases, smaller nanopores are filled, and eventually at 28 MPa the infiltration is nearly complete. As the pressure is lowered, defiltration begins at 3.2 MPa. Note that the measured defiltration plateau is also of a finite slope, which, again, should be related to the pore size distribution. That is, defiltration in smaller nanopores is easier than in larger nanopores, since the capillary ‘driving force’ of liquid motion is higher and the energy barrier of gas phase nucleation is lower [18].

A remarkable phenomenon is that although the most dominant characteristic of this system, the solid–liquid

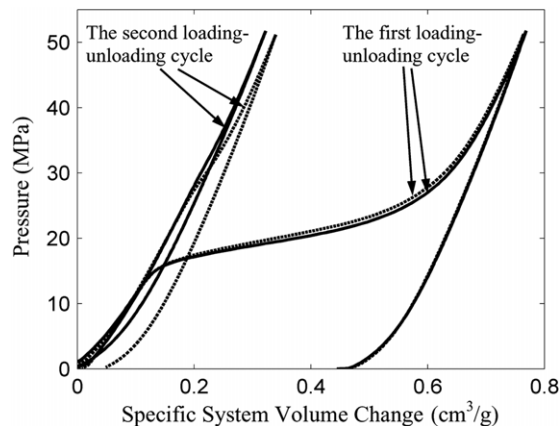


Figure 2. The dashed lines are the sorption isotherm curves of the pure water-based system and the solid lines are the sorption isotherm curves of the 10 wt% carbamide-modified system.

interfacial tension, is insensitive to the addition of carbamide, the defiltration volume, which can be estimated as the second-cycle infiltration plateau width $V_d = 0.04 \text{ cm}^3 \text{ g}^{-1}$, is largely reduced by about 67% compared with the defiltration volume $V_d = 0.12 \text{ cm}^3 \text{ g}^{-1}$ of the pure water-based system. It can be seen that the second-cycle infiltration pressure is much higher than that in the first cycle, close to the high-pressure section of the first-cycle infiltration plateau, suggesting that the reversible part of the confined liquid is in the smallest nanopores. With the addition of carbamide, since p_{in} does not vary much, the ‘driving force’ of defiltration caused by the capillary effect of the lyophobic nanopore surface remains the same. Thus, the decrease in the defiltration volume should be associated with the increase in gas solubility. The two amino groups in the carbamide molecule can promote the formation of molecular clusters of gas and liquid species, and therefore more gas molecules can be dissolved in the carbamide modified liquid phase [19]. It is assumed that as a ‘structure breaker’ carbamide disrupts the structure of water by setting up new hydrogen bonds when a cavity is produced to accommodate the solute [20]. As a result, in a nanopore, the energy barrier of gas phase nucleation increases, and even under a relatively low pressure the confined liquid does not come out.

As the carbamide concentration is increased to 20 wt%, as shown in figure 3, while V_{in} shows no significant change, the decreases in $p_{in} = 14.0 \text{ MPa}$ and $V_d = 0.02 \text{ cm}^3 \text{ g}^{-1}$ become more pronounced. The change in V_d is 83% compared with $V_d = 0.12 \text{ cm}^3 \text{ g}^{-1}$ of the pure water-based system. The variation in p_{in} , while still secondary compared with the change in V_d , is about 12.5% compared with $p_{in} = 16.0 \text{ MPa}$ of the pure water-based system, leading to a lower capillary ‘driving force’ of defiltration. The defiltration volume, V_d , is almost zero. In such a NEAS, the energy absorption is complete and no liquid would be ‘bounced back’ after the first unloading.

Figure 4 shows the sorption isotherm curves of the NEAS modified by 2 wt% SBS. Unlike the carbamide-modified system, the infiltration volume $V_{in} = 0.39 \text{ cm}^3 \text{ g}^{-1}$ is smaller than that of the pure water-based system by about 13.3%. Moreover, the infiltration pressure, $p_{in} = 15.0 \text{ MPa}$, is reduced by 6.3% compared with the pure water-based system, especially in the beginning section of the

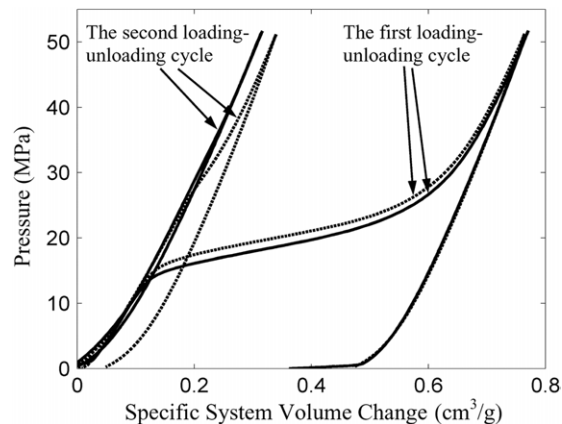


Figure 3. The dashed lines are the sorption isotherm curves of the pure water-based system and the solid lines are the sorption isotherm curves of the 20 wt% carbamide-modified system.

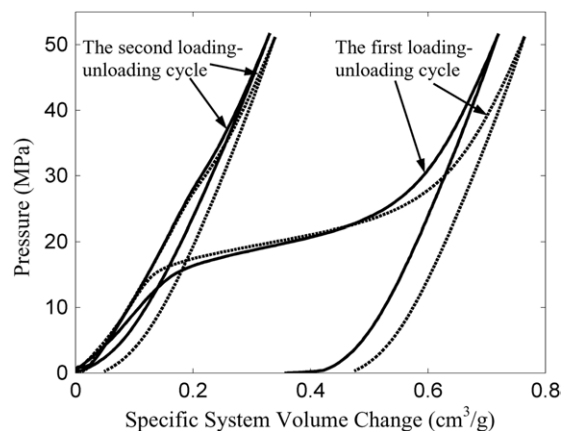


Figure 4. The dashed lines are the sorption isotherm curves of the pure water-based system and the solid lines are the sorption isotherm curves of the 2 wt% SBS-modified system.

infiltration plateau. That is, in the relatively large nanopores the infiltration can be promoted by the SBS molecules, since they are effectively wetting on the nanopore surfaces. In the relatively small nanopores, the promotion effect on infiltration is less pronounced. Particularly, in the smallest nanopores associated with the high-pressure end of the infiltration plateau, infiltration cannot take place, resulting in the reduced V_{in} . According to previous experimental data [17] and molecular dynamics simulations [1], the admixture molecule demands a free volume several times larger than itself to enter a nanochannel; otherwise the repelling effect, even for nominally wettable nanochannel walls, would be dominant.

When the SBS concentration is increased to 20 wt%, these effects become more significant, as shown in figure 5. Compared with the pure water-based system, the infiltration pressure, $p_{in} = 11.9 \text{ MPa}$, is considerably reduced by 25.6% compared with the pure water-based system. The defiltration volume is almost zero. Note that the decrease in the infiltration volume is about the same as the decrease in the defiltration volume, suggesting that most of the smallest nanopores in which the confined liquid motion is reversible are deactivated. Thus, the system exhibits a similar nonoutflow characteristic as the carbamide-modified system.

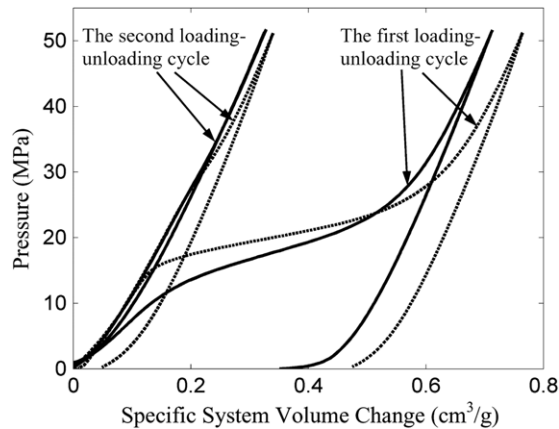


Figure 5. The dashed lines are the sorption isotherm curves of the pure water-based system and the solid lines are the sorption isotherm curves of the 20 wt% SBS-modified system.

4. Concluding remarks

Through a pressure-induced infiltration experiment on carbamide- and SBS-modified systems, it was validated that using admixtures can significantly influence the motions of confined liquids in lyophobic nanoenvironments. Although the total energy absorption capacity may slightly decrease, the risk of defiltration of the pressurized liquid is minimized. The following conclusions are drawn.

- (1) Addition of carbamide in the nanoporous silica gel-based system has little influence on the infiltration pressure and the infiltration volume, while it can considerably reduce the defiltration volume.
- (2) As the carbamide concentration reaches 20 wt%, the defiltration volume is nearly zero. The suppression effect on defiltration should be attributed to the increase in the energy barrier of gas phase formation and growth.
- (3) Addition of SBS in the nanoporous silica gel-based system can considerably reduce the infiltration pressure in the relatively large nanopores and suppress infiltration in the smallest nanopores.

- (4) The reversible part of confined liquid vanishes as the SBS concentration reaches 20 wt%. The reduction in the defiltration volume can be attributed to the blocking effect of SBS molecules in the smaller nanopores.

Acknowledgments

This work was supported by The Army Research Office under Grant No W911NF-05-1-0288, for which the authors are grateful to Dr D M Stepp.

References

- [1] Wasan D T and Nikolov A D 2003 *Nature* **423** 156
- [2] Sansom M S P and Biggin P C 2001 *Nature* **414** 156
- [3] Hummer G, Rasaiah J C and Noworyta J P 2001 *Nature* **414** 188
- [4] Birenbaum N S, Lai B T, Chen C S, Reich D H and Meyer G J 2003 *Langmuir* **19** 9580
- [5] Gomez J A and Thompson W H 2004 *J. Phys. Chem. B* **108** 20144
- [6] Kong X, Surani F B and Qiao Y 2005 *J. Mater. Res.* **20** 1042
- [7] Surani F B, Kong X, Panchal D B and Qiao Y 2005 *Appl. Phys. Lett.* **87** 163111
- [8] Desbiens N, Boutin A and Demachy I 2005 *J. Phys. Chem. B* **109** 24071
- [9] Walther J H *et al* 2004 *Carbon* **42** 1185
- [10] Majumder M, Chopra N, Andrews R and Hinds B J 2005 *Nature* **438** 44
- [11] Lefevre B, Saugey A, Barrat J L, Bocquet L, Charlaix E, Gobin P F and Vigier G 2004 *Colloids Surf. A: Physicochem. Eng. Asp.* **241** 265
- [12] Hull J B 1992 *Br. J. Surg.* **79** 1303
- [13] Wightman J M and Gladish S L 2001 *Ann. Emergency Med.* **37** 664
- [14] Chaloner E 2005 *British Med. J.* **331** 119
- [15] Kong X and Qiao Y 2005 *Phil. Mag. Lett.* **85** 331
- [16] Kong X and Qiao Y 2005 *Appl. Phys. Lett.* **86** 151919
- [17] Surani F B, Kong X and Qiao Y 2005 *Appl. Phys. Lett.* **87** 251906
- [18] Han A, Kong X and Qiao Y 2006 *J. Appl. Phys.* **100** 014308
- [19] Yalkowsky S H 1999 *Solubility and Solubilization in Aqueous Media* (Oxford: Oxford University Press)
- [20] Breslow R and Guo T 1990 *Proc. Natl Acad. Sci.* **87** 167